Global Journal of Pure and Applied Mathematics.
ISSN 0973-1768 Volume 12, Number 1 (2016), pp. 657-676

http://www.ripublication.com

Formation of a Secondary Current Signal in Electron Beam Welding of Dissimilar Materials

Dmitriy Nikolaevich Trushnikov
Perm National Research Polytechnic University, Komsomolsky Av., 29, Perm, Perm Krai, 614990, Russia.

Vladimir Yakovlevich Belenkiy
Perm National Research Polytechnic University, Komsomolsky Av., 29, Perm, Perm Krai, 614990, Russia.

Ekaterina Sergeevna Salomatova
Perm National Research Polytechnic University, Komsomolsky Av., 29, Perm, Perm Krai, 614990, Russia.

Abstract

The article explores the formation of a secondary current signal depending on the welded material during electron beam welding of dissimilar materials (namely, high-strength steel with copper and copper alloys). The article primarily focuses on the fundamental aspects of the interaction of a powerful concentrated electron beam with welded metal during electron beam welding. Application of the synchronous storage method during electron beam welding with beam oscillation across the joint makes it possible to evaluate the formation of a signal in the process of interaction with each particular material. The obtained results can be useful in developing models of the formation of plasma and secondary current in the plasma during electron beam and laser welding, as well as in developing models of electron beam welding of dissimilar materials. Besides, the obtained results can be the basis for the development of methods of on-line monitoring of electron beam deflection during beam welding of dissimilar metals.

Keywords: highly concentrated heating sources, electron beam welding of dissimilar materials, method of on-line monitoring of an electron beam.

Introduction

An important problem in the development of fault-free technology of electron beam welding is to ensure reproducible quality of welded joints. Research on automation of

this process using the parameters of secondary current signals has been carried out for long enough with variable success [1,2,3,4,5]. So far, however, the problem has not been solved yet. Some progress has been achieved by using methods based on the detection of secondary X-ray emission generated during electron beam welding [3,4]. However, these methods have certain limitations, resulting from the difficulty of placing additional sensors in the vacuum chamber, which causes difficulties when using them in industrial environments. In addition, a number of studies show that electron beam welding is accompanied by high-frequency oscillatory processes [6,7], which in some cases carry essential information concerning the thermal characteristics of the interaction of an electron beam with metal in the keyhole. Similar phenomena are also observed in laser welding [8]. These processes proceed with a frequency of $2 \cdot 10^4$ Hz, which makes it difficult to detect them using X-ray sensors. Methods based on the detection of secondary current in the plasma generated over the area of electron beam welding are the most promising in this respect [9], [10]. At the same time, it should be noted that the task of controlling penetration during electron beam welding using parameters of the secondary current in the plasma cannot be considered to be solved. There are no models that describe the relationship between the parameters of the secondary current signals in the plasma and the characteristics of the thermal effect of an electron beam. Thus far, no universal, reliable and fast-response weld control systems applicable for electron beam welding have been developed. The accumulated data are often tentative.

Recent research [6,11,12], have shown the prospects of the application of the synchronous storage method for studying processes taking place in the keyhole during electron beam welding. The result of synchronous storage makes it possible to analyze how the processes in the keyhole synchronize with the signals in the deflecting or focusing coils of an electron gun. It was found that the secondary current signal is displaced in phase in relation to the signal of the deflecting coils. And, in this case, it is not the result of the thermal inertia of the process, as the sign of the phase shift changes after transition from the regime with an underfocused electron beam to the regime with an overfocused beam. This fact is of particular interest, because its interpretation will allow for a better understanding of the essence of the processes taking place in the keyhole and the mechanism of the formation of a secondary current signal in the plasma.

The results of the research on electron beam welding of different materials are very important for development of models. Comparison of these results will make it possible to determine the role of various factors influencing the secondary current parameters.

This article explores the formation of a secondary current signal depending on the welded material during electron beam welding of dissimilar materials (namely, high-strength steel with copper and copper alloys). Problems of weldability of these materials are the subject of special study and are discussed in [13]. This article primarily focuses on the fundamental aspects of the interaction of a powerful concentrated electron beam with welded metal during electron beam welding. Application of the synchronous storage method during electron beam welding with beam oscillation across the joint makes it possible to evaluate the formation of a

signal in the process of interaction with each particular material. The obtained results can be useful in developing models of the formation of plasma and secondary current in the plasma during electron beam and laser welding, as well as in developing models of electron beam welding of dissimilar materials. Besides, the obtained results can be the basis for the development of methods of on-line monitoring of electron beam deflection during beam welding of dissimilar metals.

Methodology

Welding was carried out using the electron beam welder with the power supply unit ELA-60/6VH produced by SELMI (Ukraine), with oscillation of an electron beam across the joint according to the saw-tooth pattern. The amplitude and frequency of the oscillation were within the range of 0.4-0.8 mm and 200-1000 Hz, respectively. For the detection of secondary current in the plasma, a non-self-maintained discharge was induced in the plasma formed in the area of concentrated electron beam exposure. For this purpose an electron collector was installed over the welding area [6,7,9]. In these experiments, the collector had a positive potential of 48V in respect to the welded item. The synchronous storage method was used for the analysis of a high-frequency component of the secondary current in the plasma [6,14]. In this experiment, welding passes were carried out in an interlocking circular joint with a diameter of 120 mm and a thickness of 8 mm, composed of copper or bronze and stainless steel 09Cr16Ni4N. A steel billet was used as a backing strip. The electron beam power in the experiments was from 2 to 2.5 kW.

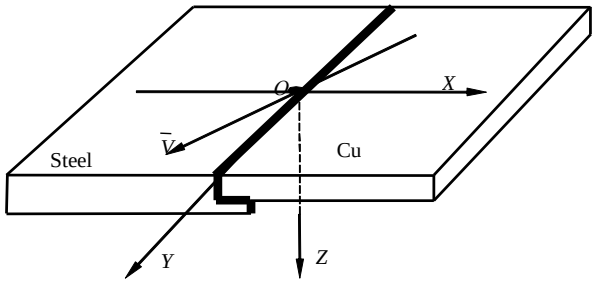

Figure 1: The diagram of making welding passes with adjustable position of an electron beam in respect to the joint

Before welding, an electron beam was pointed with a shift in relation to the joint of welded billets, and progressive transverse shifting of the beam was carried out while making welding passes (Fig. 1). Thus, the results for different beam positions in relation to the joint were obtained during one welding pass. Welding passes were made with full penetration of the metal. The welding speed was 5 mm/s.

The implementation of the synchronous storage method was carried out in accordance with the flowchart shown in Fig. 1. A reference square signal *g(t)* with a low pulse ratio and with a period *T* was formed out of periodic signal of deflecting coils *Osc(t)*

with the same period. The reference signal $g(t + \tau)$ shifted in relation to the received signal $Osc(t)$ for a specified time interval τ.

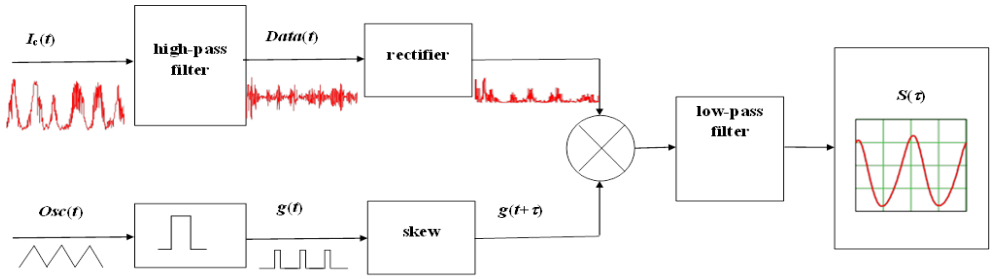

Figure 2: The diagram of the implementation of the synchronous storage method [7]

The signal of the secondary current in the plasma $I_k(t)$was processed using a digital or analog high-frequency filter with a cutoff frequency of about 10 kHz. The high frequency component of the received signal $Data(t)$ was rectified and then multiplied by the base signal $g(t+\tau)$. The result was then integrated over the time:

$$S(\tau) = \int_0^{t_0} g(t+\tau) \cdot \left| Data(t) \right| dt$$

where t_0 is the reference time.

The function $S(\tau)$ is the average amplitude of the high frequency secondary current signal for each shift value τ. With respect to the processing of the signal of the secondary current in the plasma during electron beam welding by an oscillating electron beam the method can be described as follows. In the keyhole there is an area of interaction of a beam with metal on the walls of the keyhole, which can be called the area of a maximum power density. In the process of oscillation of an electron beam this area moves along the walls of the keyhole. Each position of this area corresponds to the average amplitude of high frequency oscillations of the secondary current. The function $S(\tau)$ may be presented in a phase space. To achieve this, the value of the current of deflecting coils $Osc(\tau)$ or the electron beam deflection in the keyhole x is plotted along the horizontal axis.

Results

Fig. 3 shows the results of the processing of the signal of the secondary current in the plasma using the synchronous detection method during electron beam welding of 09Cr16Ni4Nb steel (Fig. 3, a) and chromium bronze (Fig. 3, b), the chemical composition of the steel and chromium bronze in a table 1. Attention should be paid to the difference of scales in these figures. Thus, the amplitude of the high frequency component of the oscillations of the signal of the secondary current in the plasma is about twice as large as that in welding of bronze. The results were obtained using different values of welding power, which was chosen to provide the same penetration depth. At the same values of the electron beam power, the difference in values of the

secondary current signal would be even greater. As the charts show, the resulting curves are of the same nature and differ only in the values of the secondary current signal. For the position, where the electron beam axis coincides with the axis of symmetry of the keyhole, the time-mean value of the secondary current signal reaches a minimum. When a beam deflects to the walls of a keyhole, the level of secondary current signal increases. In both cases the curves are characterized by a phase shift (lag) of the secondary current signal in relation to the current of the deflecting coils. The existence of this lag was noted in [6]. Experiments have shown that the value of this lag is much more important for bronze welding than for steel welding. The nature of the lag and its dependency on the electron beam welding conditions will be discussed in more detail in subsequent works. For the curves shown in Fig. 3 the values of the secondary current signal were averaged separately in the process of forward movement in the direction of welding and in the process of backward movement. One can calculate the mathematical expectation using the value of semi-oscillation, which will be done in further experiments for the ease of interpretation.

Table 1: The chemical composition of 09Cr16Ni4Nb steel [15] and chromium bronze [16]

No.	1	2	3	4	5	6	7	8
Chemical element 09Cr16Ni4Nb steel	Cr	C	Si	Mn	Ni	Nb	P	S
Percentage	15.0-16.5	0.08-0.12	0.6	0.5	4.0-4.5	0.05-0.15	0.03	0.015
Chemical element chromium bronze	Fe	Cr	Cu	Zn	-	-	-	-
Percentage	0.08	0.4-1.0	98.5-99.6	0.3	-	-	-	-

Steel	Steel-Cu
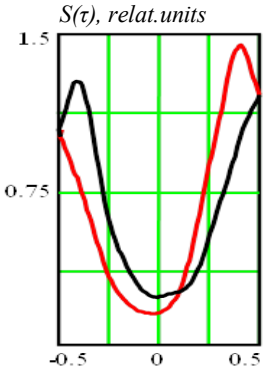	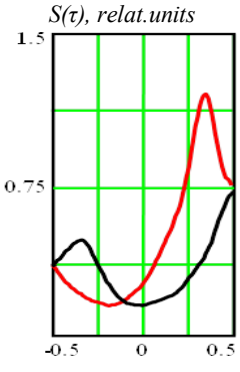
x = -3 mm	x=-0.6 mm
a)	*b)*

Steel-Cu	Steel-Cu
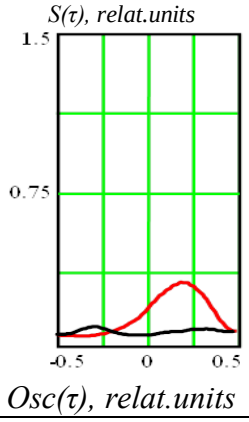	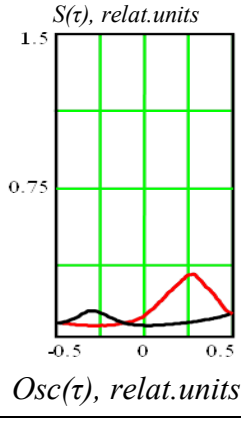
x= 0mm	x = -2 mm
c)	*d)*
Cu	
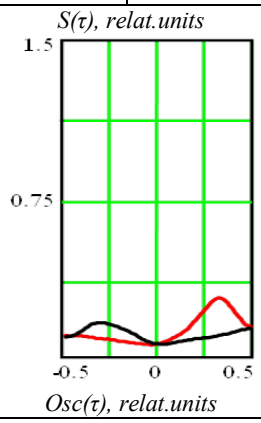	
x = 3 mm	
e)	

Figure 3: The result of the processing of the secondary current signal using the method of synchronous storage (weld pass from steel to copper, fine focus ΔI_f = 0 mA, *x* – mean beam deflection in relation to the joint in the process of its oscillation (the beginning of the axis is at the joint, the direction is toward copper), the right side of the curves corresponds to the deflection in the direction of copper)

Somewhat unexpected results were obtained when analyzing the formation of a secondary current signal while changing the electron beam shift in relation to the joint. It was assumed that taking into account the received data for the formation of a signal during independent passes in steel and copper (or bronze), in case of electron beam deflection from steel to copper (bronze) the signal value should decrease. The shape of the curve obtained by the method of synchronous storage in welding along the joint should be asymmetrical with reduction on the part of copper (bronze). However, the results of the experiments did not confirm these assumptions. Figures 4

and 5 shows the results obtained when passing from steel to copper and from bronze to steel (Fig. 5).

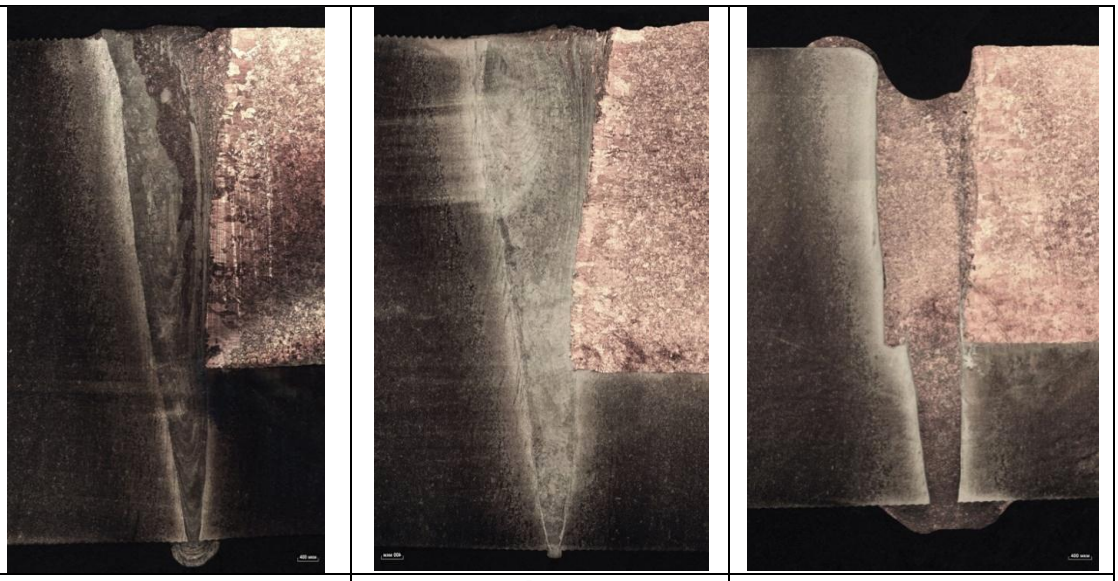

a) b) c)

Figure 4: The macrostructure of the welds of steel 09Cr16Ni4Nb and copper: a – deflection of an electron beam to steel (x = -1 mm); b – movement of an electron beam along the joint between steel and copper (x = 0 mm); c – deflection of an electron beam to copper (x = 1.5 mm); magnification of 400.

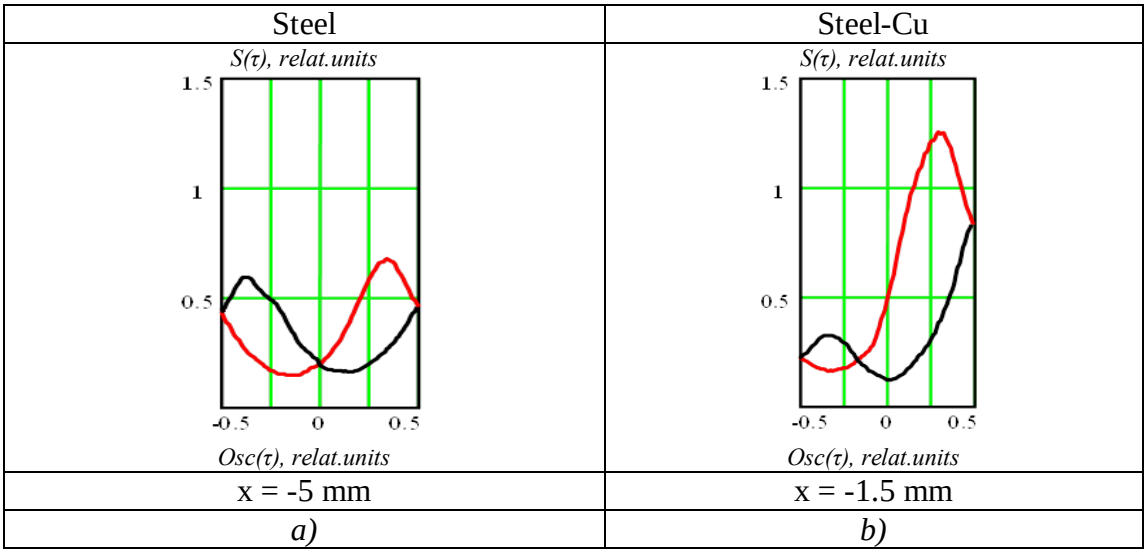

Steel-Cu	Steel-Cu
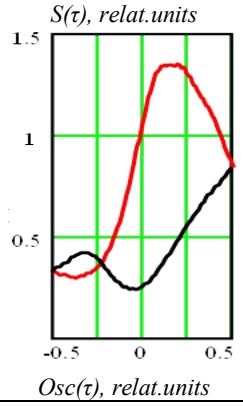	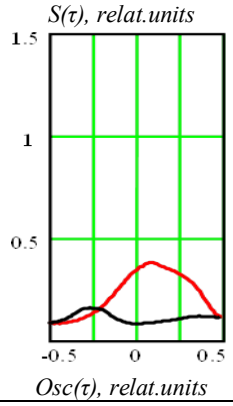
x = -0.4 mm	x = 1.3 mm
c)	*d)*
Cu	
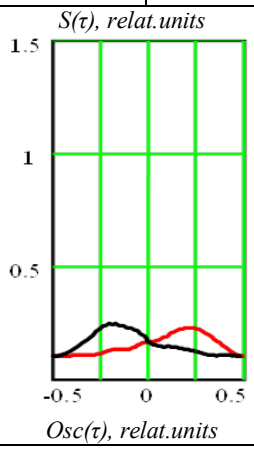	
x = 5 mm	
e)	

Figure 5: The result of the processing of the secondary current signal using the method of synchronous storage (weld pass from bronze to steel, underfocused mode – ΔI_f = -5 мА, *x* – mean beam deflection in relation to the joint in the process of its oscillation (the beginning of the axis is at the joint, the direction is towards bronze), the right side of the curves corresponds to the deflection in the direction of bronze)

One can see that when an electron beam shifts from steel to copper (bronze), the value of the secondary current signal is reduced. However, the asymmetry of the received curves differs significantly from the expected asymmetry. When welding steel the shape of the curve is almost symmetrical (Fig. 4, a). As an electron beam shifts towards copper and its melt gets into the weld pool, the symmetry is broken. Thereat, instead of reducing of the signal level at the time when the oscillating bean is shifted towards copper, it is the reverse. The signal in this case practically doesn't change (Fig. 4, b) (or even increases – Fig. 6, b). At the same time, when the electron beam is

on steel the signal drops rapidly. Thereafter, when passing the joint (Fig. 4, c, d, Fig. 6, c, d) the asymmetry persists, the overall signal level is reduced. In case of shifting of an electron beam, which performs only penetration of copper (bronze), the curves become symmetric again (Fig. 4, e, Fig. 5, e).

The value of the secondary current signal in the plasma during electron beam welding depends to a greater or lesser degree on many factors, in particular, on the characteristics of the materials (thermophysical properties, electronic work function, etc), technological parameters of welding (electron beam power, welding speed, frequency and amplitude of beam oscillation, etc.), the geometry of the keyhole and the temperature in the area of interaction of an electron beam with metal. The data on the geometry of the keyhole can be received indirectly, by analyzing the shape of penetration on the macro slices of penetration areas produced after welding. However, for the interpretation of the obtained results it is necessary to estimate temperatures in the keyhole when welding dissimilar materials.

Discussion

A. The mathematical model for calculation of the temperature in the keyhole during electron beam welding of dissimilar metals

The model is based on the analysis of the balance of an element of the keyhole wall in the metal. Vapor pressure is balanced by the surface tension forces and hydrostatic pressure in the molten pool [14].

$$P = \rho g h + \frac{\sigma}{r}$$

where P is the vapor pressure on the walls of a keyhole, ρ is the density of the material; h is the depth of a keyhole; σ is the surface tension of the material; r is the radius of a keyhole.

Thermodynamic calculation of vapor pressure in the keyhole during electron bean welding of alloys is based on the determination of the total vapor pressure (P_{total}) in the keyhole, which is the sum of the partial pressures of the alloy elements (P_i) [22]:

$$P_{total} = \sum_{1}^{n} P_i$$

$$P_i = P_i^0 \cdot a_i$$

where P_i^0 is the partial pressure of the saturated vapor of the i^{th} element over the pure element, which can be represented in the form of the Clapeyron-Clausius equation:

$$\lg P_i^0 = -\frac{\Delta H_{vap,i}}{2.3 \cdot RT} + B_i,$$

where $\Delta H_{vap,i}$ is the enthalpy of vaporization of the i^{th} element; R is the gas constant; B is the constant for the given temperature range.

The activity of the alloy's elements is determined by the formula:

$$a_i = X_i \cdot \gamma_i$$

where X_i is the atomic ratio of the i^{th} element; γ_i is the activity coefficient of the i^{th} element in the alloy.

Vapor pressure, thus, depends on the chemical composition of the welded alloy. During electron beam welding of a dissimilar joint with oscillation of a beam across the joint, the electron beam during the period of oscillation will for some time interact with one material, while interacting with another material for the rest of the time. These time values are determined by the average deflection of a beam in relation to the joint. Evaporation in this case will take place in the same manner, as if the electron beam acted upon the alloy of two materials in a certain proportion. Table 2 shows an example of the averaged chemical composition of the alloy received after crystallization of the welding bath during electron beam welding of 09Cr16Ni4Nb steel and copper (the chemical composition of 09Cr16Ni4Nb steel and chromium bronze to be in table 1) for a welding pass with a minimum deviation from the joint.

Table 2: The averaged chemical composition of the weld metal during electron beam welding of dissimilar joint of 09Cr16Ni4Nb steel and copper

No.	1	2	3	4	5	6	7
Chemical element	Fe	C	Si	Mn	Ni	Cr	Cu
Percentage	44.7	0.05	0.3	0.25	2.1	8.0	44.6

All the calculations were performed in Mathcad. The results of the calculations according to the formulae given above are presented in the form of charts in Fig. 6.
The charts show that copper makes the most significant contribution to the vapor pressure in the keyhole, chromium and iron make insignificant contributions. The contribution of other elements to the vapor pressure in the keyhole can be ignored.
The surface tension and density of molten metal in the first place depend on the temperature. With the rise in temperature the density and surface tension are reduced. So it is important to accurately determine the values of these parameters at the specified temperature of the melt. To determine the density of the material we used the experimental data provided in the reference literature. To determine the surface tension of the alloy of steel and copper we used the calculation formula proposed by Volkmann [17]:

$$\sigma_{St}^{T} = \sum \sigma_i^T \cdot X_i \qquad (1)$$

where σ_i is the surface tension of the i^{th} component in the alloy, X_i is the nuclear fraction of the i^{th} component in the alloy.

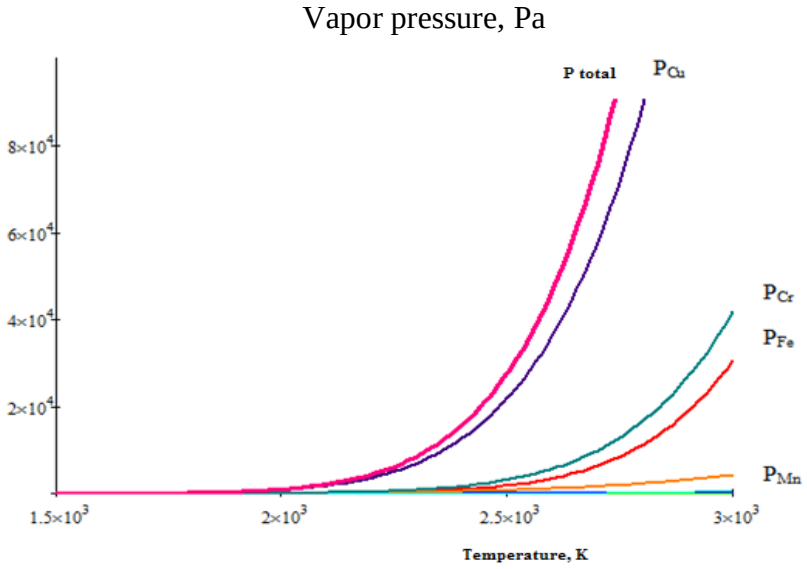

Figure 6: The curve of the vapor pressure in the keyhole against temperature: 1 – Fe, 2 – C, 3 – Si, 4 – Mn, 5 – Ni, 6 – Cr, 7 –Cu, P_{total} –the total vapor pressure in the keyhole

To determine the surface tension σ_i of the i^{th} component in the alloy we used the equation (2) proposed by S.I. Popel [18]:

$$\sigma_i^T = \sigma_0 + \left(\frac{\partial\sigma}{\partial T}\right) \cdot (T - T_m) \qquad (2)$$

where σ_0 is the surface tension of metals at a temperature of 20° C, $\left(\frac{\partial\sigma}{\partial T}\right)$ is the temperature coefficient, Tm is the metal melting point (see Table 2).

Table 2: The surface tension of alloy components and their temperature coefficients

Metal	T_m, K	**σ_0,** mJ/m^2	$-\left(\frac{d\sigma}{dT}\right)$, mJ/(m^2·K)
Fe	1823	1860	0.35
Mn	1573	1050	0.25
Ni	1773	1750	0.34
Cr	2103	1540	0.20
Cu	1373	1350	0.17

Using the formulae 1 and 2 and the data of the Table 2, we get the temperature dependence of the surface tension of the alloy of steel 09Cr16Ni4Nb and copper (Fig. 7).

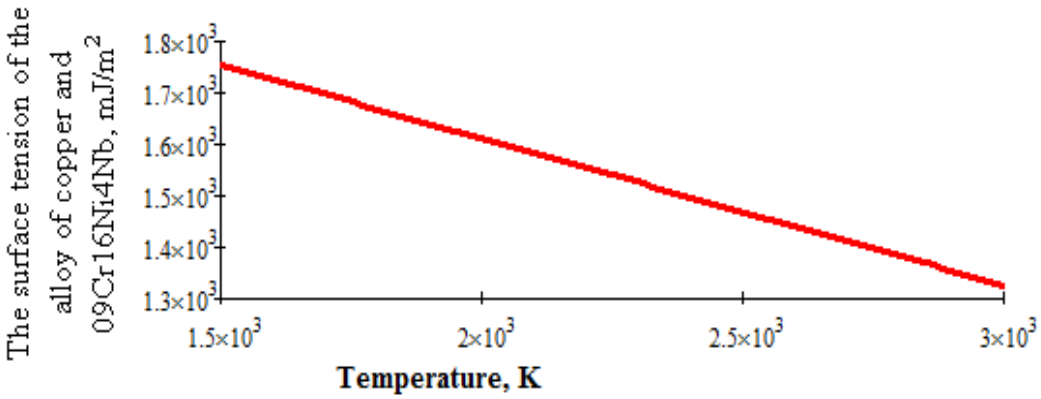

Figure 7: The curve of the surface tension of alloy of 09Cr16Ni4Nb steel and copper against temperature

A keyhole in electron beam welding has a complex shape, which changes over time. Assuming the smallness of the ratio of the radius of the keyhole to its depth, we approximate the keyhole by a cylinder with a hemispherical bottom (Fig. 8). Let us make calculations for the penetration depth h = 7 mm. The radius of the keyhole in the first approximation is taken to be equal to the radius of the electron beam $r = r_b$ = 0.3 mm.

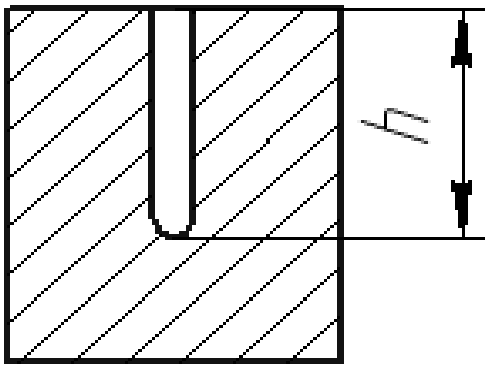

Figure 8: Schematic layout of a vapor-gas channel in the liquid metal in electron beam welding

The calculated total pressure of the hydrostatic forces and surface tension forces for the alloy of 09Cr16Ni4Nb steel and copper is presented in the Table 3.

Table 3: The total pressure of the hydrostatic forces and surface tension forces for the alloy of 09Cr16Ni4Nb steel and copper

Temperature, K	1850	2000	2300	2600	2900
Vapor pressure, Pa	$5.29 \cdot 10^4$	$5.16 \cdot 10^4$	$4.90 \cdot 10^4$	$4.64 \cdot 10^4$	$4.38 \cdot 10^4$

The temperature in the keyhole is determined by the equality of the vapor pressure and the pressure in the liquid (Fig. 9). The equality of the vapor pressure in the keyhole and the pressure in the liquid phase defines the integral temperature in the keyhole. For the alloy of 09Cr16Ni4Nb steel and copper, under given conditions, the integral temperature at the bottom of the keyhole is 2,429 K. Similarly, it is possible to calculate the temperature of the walls of the keyhole (Fig. 10) and the vapor pressure (Fig. 11) at an arbitrary depth, for which purpose it is necessary to substitute depth *z*, measured in relation to the surface of the welded item, for the keyhole depth *h* in the formula (1).

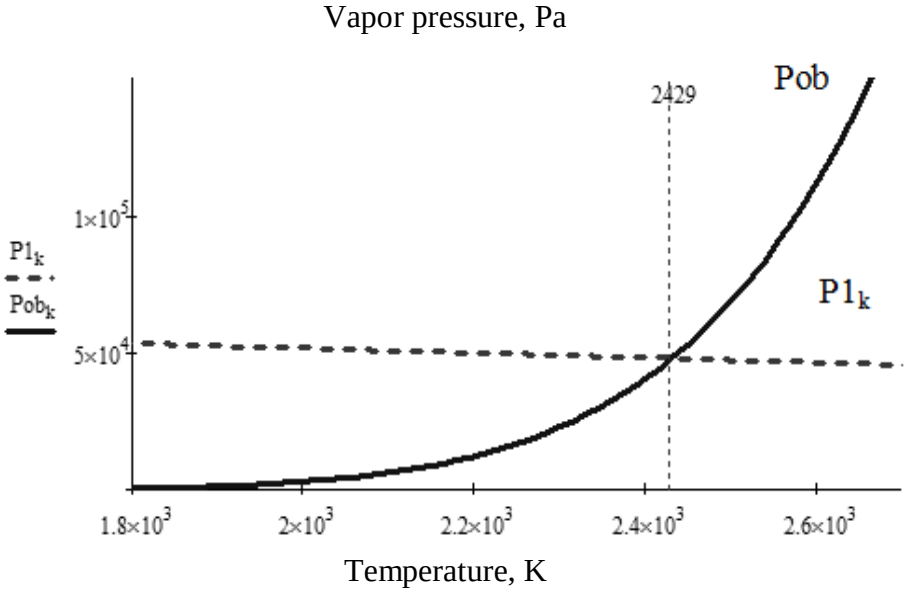

Figure 9: The curve of the vapor pressure in the keyhole and the pressure in the liquid phase for the alloy of 09Cr16Ni4Nb steel and copper against temperature: P_{ob} is the vapor pressure in the keyhole, $P1_k$ is the total pressure-of the hydrostatic forces and surface tension forces on the surface of the molten pool

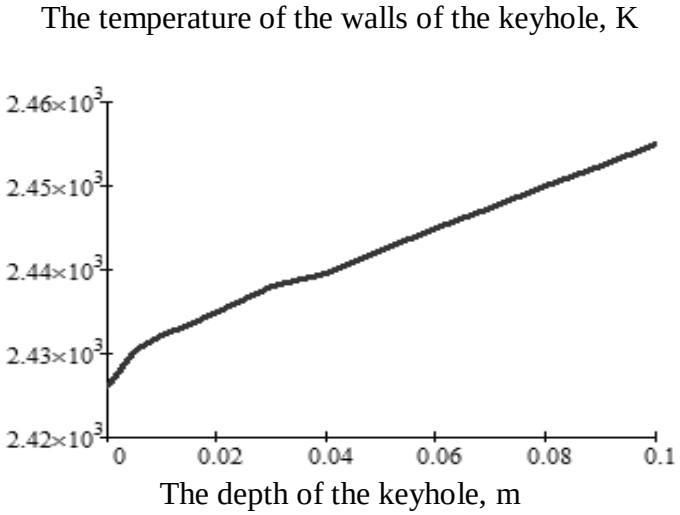

Figure 10: The curve of the temperature against the depth of the keyhole during electron beam welding of 09Cr16Ni4Nb steel and copper

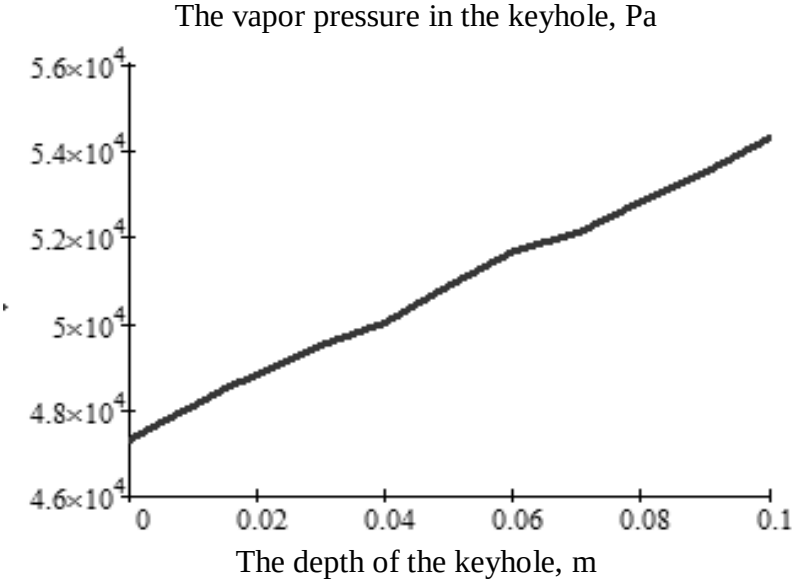

Figure 11: The curve of the vapor pressure in the keyhole against the depth of the keyhole during electron beam welding of 09Cr16Ni4Nb steel and copper

The charts show that, given the assumptions made, with an increase in the depth of the keyhole the temperature rises insignificantly (by less than 2%). At the same time in the works [19, 20, 21, 22], the essential difference (about 20%) is shown between the temperatures at the bottom and on the surface of the keyhole. Thus, we can say that the model described above is an estimation model, and the accuracy of the results obtained by using this model doesn't exceed 10%. This may be due to the following.

The proposed calculation did not take into account changing of the radius of the keyhole depending on its depth. Under actual welding conditions, the radius of the keyhole slightly increases with the decreasing of the depth, which should lead to the additional increase of the temperature at the bottom of the keyhole, compared with the received data. The smaller the depth of the keyhole, the greater the influence of this factor. The work [20] shows the results for the keyhole which is twice or three times as deep as the keyhole in the described case, which leads to different results. The greater the depth of penetration, the more feasible the approximation of the shape of the keyhole using a cylinder, and the closer the results to real data. Besides, the accuracy of this model is quite sufficient to explain the specifics of the formation of a secondary current signal in the plasma during electron beam welding of dissimilar metals.

B. The formation of a secondary current signal in electron beam welding of dissimilar metals

The use of the received model for the calculation of temperature makes it possible to estimate the dependence of the integral temperature of the walls of the keyhole on the percentage of copper in the alloy with 09Cr16Ni4Nb steel received in the process of crystallization of the molten pool (Fig. 12). With the increase of the percentage of copper in the alloy the temperature of the walls of the keyhole is reduced. Thus, the superheat of approximately 400 K is observed when welding steel with copper compared to the situation when the electron beam melts only the copper. The steel temperature is in this case lower than the initial temperature by about 400 K. In the process of the transverse oscillation of the electron beam the area of its interaction with the metal moves in a reciprocating manner on the sidewalls of the keyhole. The area of a maximum power density within the keyhole moves with the movement of the electron beam. All the previous calculations were related to some averaged temperature in the keyhole. But it is logical to expect that in a first approximation the decrease (or increase) of the temperature in the keyhole as a whole by a certain value leads to a similar temperature change by the value of the same order in the area of the interaction of an electron beam with metal.

The value of thermionic emission from the surface of the metal in the area of interaction is calculated by the Richardson-Dushman equation and is largely determined by the work function and temperature.

$$j = A \cdot T^2 \cdot \exp\left(-\frac{e\phi_o}{kT}\right),$$

where j is the density of the thermionic current, A is the Richardson constant, T is the temperature of the emitting surface; $e\phi_o$ is the electronic work function; k is the Boltzmann constant.

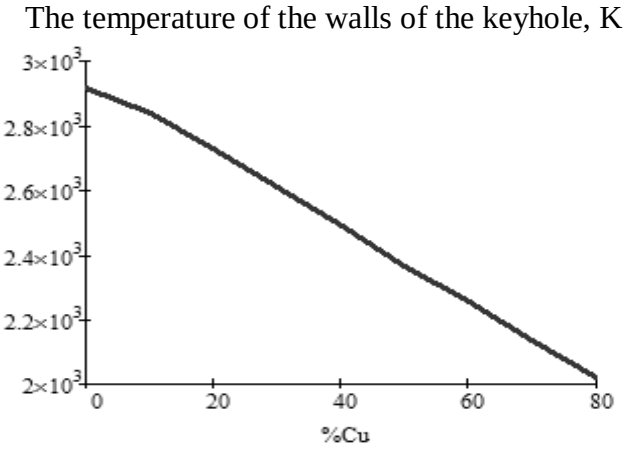

Figure 12: The curve of the temperature of the walls of the keyhole against the percentage of copper in the alloy with 09Cr16Ni4Nb steel

The reference data on the electronic work function of copper provide a range of values of 4.3…4.5 eV, for iron – 4.40…4.71 eV (the same range of values is provided for chromium). Thus, in a first approximation, one can consider the electronic work functions to be the same for all the elements. In this case, the difference in the intensity of the thermionic emission will be completely determined by the temperature in the keyhole. Let us estimate the values of the thermionic current density during electron beam welding of steel, copper, as well as in case of penetration of a steel-copper joint. In case of penetration of a steel-copper joint estimates should be made separately for steel and copper at the temperature that characterizes the keyhole. The results for different temperatures are summarized in Table 4.

Along with the values of the thermionic current density, Table 4 shows the magnitudes of thermionic currents. Experiments [5,8], show that in electron beam welding with oscillation, the area of a maximum power density (the area of thermionic emission) is localized in the area interaction of an electron beam with metal. During welding this area randomly moves up and down along the front wall of the keyhole. During electron beam welding with oscillation this movement becomes regular. Accordingly, in the calculations the area of the emitting surface was taken to be equal to the beam cross section (the radius of the beam was taken to be 0.3 mm). It must be remembered that what is meant here is the assessment of density of the thermionic current from the area of the interaction of an electron beam with metal, and not the current detected by the electron collector located over the welding area. In case of the measurement of this current by the collector the current magnitude is influenced by a number of factors – the shape and size of the keyhole, the conditions of the flowing of the secondary emission current in the plasma, the position of the area of the interaction of an electron beam with metal, the position of the minimum diameter of the electron beam in the depth of the keyhole, etc. However, plasma, as a good conductor, passes the most part of the thermionic current to the collector.

Table 4: The density of the secondary current and the current itself during welding of steel and copper

Metal (alloy)	T, K	$e\phi_o$, eV	(j), A/m^2	I, A
steel	2800	4.6	$50 \cdot 10^3$	0.014
	3200		$710 \cdot 10^3$	0.2
copper	2000	4.32	63	10^{-5}
			$318 \cdot 10^3$	0.09
steel when welded with copper	2400	4.6	$1.5 \cdot 10^3$	$4 \cdot 10^{-4}$
	2800		$100 \cdot 10^3$	0.029
copper when welded with steel	2400	4.32	$40 \cdot 10^3$	$1.7 \cdot 10^{-3}$
	2800		$600 \cdot 10^3$	0.171

The measured current in the plasma is the current of a non-self-maintained discharge in the plasma. Fig. 13 shows the diagram of generation and measurement of the current of a non-self-maintained discharge in the plasma over the molten pool. A concentric electrode (collector 4) is placed upon the section of an electron gun. The voltage potential of +50 V, which is significantly greater than the voltage potential of the plasma in the current take-off area, is applied to the collector from the constant voltage source 7 through the load resistance. The current I_e, which is the current of a non-self maintained arc discharge and flows due to thermionic emission from the most heated areas on the walls or at the bottom of the keyhole, flows through the circuit: constant voltage source 7, load resistance 6 (about 50 ohms), collector 4, plasma column 3, welded sample 8, earth.

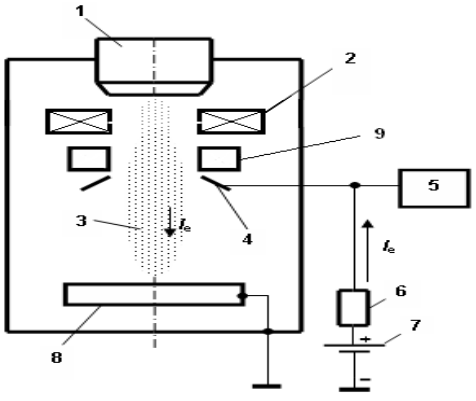

Figure 13: The diagram of the measurement of the current of a non-self-maintained arc discharge: 1 – electron gun, 2 – focusing system, 3 – plasma, 4 – plasma current collector, 5 – measuring system for data processing, 6 – resistance, 7 – constant voltage source, 8 – sample, 9 – deflecting system

Of course, the current will only flow in the collector circuit under condition of sufficient emission capacity of the cathode, following its change. Along with the

thermionic emission, the electrons which are reflected from the metal and the secondary high energy electrons also make some contribution to the collector current. It is possible that the secondary emission induced by the bombardment of the metal with ions which are accelerated by the strong electric field near the surface of the metal (the cathode), also has some effect, but its role in the arc discharge is minimal. The insignificant effect of reflected and secondary electrons is confirmed by the nature of the oscillograms of the secondary current in the plasma [6]. The secondary current is a series of high-frequency impulses, between which the signal value drops to almost zero. Moreover, this fact confirms that the pulses are caused not by the temperature of the keyhole in general, but by the superheat of certain areas, that is, the area of thermionic emission is localized in space.

This is confirmed by the data in the Table 4. At the integral temperatures obtained in the course of modeling for steel (2,800 K) and bronze (2,000 K) the magnitudes of thermionic currents are by an order of magnitude lower than those observed experimentally. To achieve the order-of-magnitude agreement, one should assume the existence of the local superheat of the metal in the area of the interaction. The data in the table 4 show that the required superheat is about 400 K. The hypothesis of the existence of such superheat accompanied by boil-offs has been proposed in many works. Experimentally, this hypothesis is confirmed by the pulse nature of secondary current signals [6], [7] and localization of the area of maximum power density. Now we have an opportunity to assess the value of these superheats.

Conclusion

The model for the calculation of temperature in the keyhole during welding of dissimilar metals, combined with the equation for the thermionic emission and supplemented with the assumption of the existence of superheats in the area of the interaction of an electron beam with the walls of the keyhole, provide, in the aggregate, the model that describes the formation of a thermionic signal. When welding steels we get temperatures of about 3,200 K in the area of interaction. The value of the pulses of the secondary current amounts in this case to approximately 0.2 A, which is in good agreement with the experimental data. When welding copper the corresponding values are 2,400 K and 0.1 A respectively. When welding dissimilar materials, an electron beam overheats the metal on the walls of the keyhole to 2,800 K. The thermionic current on the part of copper reaches in this case 0.171 A, while on the part of steel it drops to 0.029 A.

It is found that the amplitude of the high-frequency oscillations of the secondary current in the plasma characterizes the thermionic emission from the area of interaction of an electron beam with metal in the keyhole and depends on the welded material. When welding copper and bronze, the amplitude is reduced by an order of magnitude as compared to its value in welding of steels. It is found that during welding steel and copper the temperature in the keyhole takes an intermediate value between its value in welding of steels and in welding of copper (or bronze). The magnitude of the secondary current in the plasma reduces on the part of steel and increases on the part of copper (bronze). It is established that the superheat value in

the area of interaction of the electron beam with the walls of the keyhole is about 400 K in relation to the integral temperature in the keyhole. A mathematical model of the formation of a secondary current signal in electron beam welding of dissimilar metals has been developed. The analysis of the variation of the parameters of the secondary current in the plasma in case of the electron beam deflection in relation to the joint has also been performed. The dependence of the parameters of the secondary current in the plasma on the electron beam deflection in relation to the joint in electron beam welding of dissimilar materials can consequently be used to develop methods of on-line monitoring.

For a complete description of the process the model of the formation of thermionic current should be supplemented with a model that describes the probability of boil-off (secondary current pulses) from the depth of the position of the area of interaction of the beam with metal in the keyhole. With this supplement, the model of the formation of secondary current of a nonself-maintained arc discharge in the plasma during electron beam welding of dissimilar materials will be complete.

Acknowledgements

The study was supported by the Ministry of Education and Science of the Russian Federation within the framework of the state order (No. 1201460538) and by the grants RFBR No. 13-08-00397A, RFBR No. 14-08-96008A.

References

[1] S. Oltean, M. Abrudean, “Advanced control of the electron beam welding”, Journal of Control Engineering and Applied Informatics, vol. 1(10), pp. 40-48, 2008.

[2] K. Olszewska, K. Friedel, “Control of the electron beam active area position in electron beam welding processes”, Vacuum, vol. 1(74), pp. 29-43, 2004.

[3] V. Laptenok, A. Murygin, D. Tikhonenko, “X-ray sensor for guiding the electron beam on the joint in electron beam welding”, Welding International, vol. 20, pp. 894-900, 2006.

[4] V. Braverman, D. Skurikhin, S. Bayakin, V. Shabanov, V. Bashenko, “Device for focusing and fusion depth controlling by characteristic x-ray during electron beam welding with modulation of focusing level”, Welding fabrication, vol. 1, pp. 16-19, 1997.

[5] S. Hiramoto, M. Ohmine, M. Sakamoto, “Development of an automatic beam focus system for electron beam welding”, Weld. Int., vol. 10, pp. 763-768, 1991.

[6] E. Koleva, “Signal emitted from plasma during electron beam welding with deflection oscillations of the beam”, Journal of Materials Processing Technology, vol. 9(214), pp. 1812-1819, 2014.

[7] D. Trushnikov, “Investigation of Processes in the Keyhole of Electron beam Welding by Monitoring the Secondary Current Signal in the Plasma. In-situ

Studies with Photons, Neutrons and Electrons Scattering II". – Switzerland:Springer International Publishing, 2014.
[8] A. Kaplan, "Local flashing events at the keyhole front in laser welding", Optics and Lasers in Engineering, vol. 68, pp. 35-41, 2015.
[9] V. Belenkiy, V. Yazovskikh, A. Zhuravlev, "Nature of the secondary current in the plasma formed in the area affected by the electron beam during welding", Phys. Chem. Mater. Treat., vol. 6, pp. 128-131, 1983.
[10] V. Vinogradov, "Using plasma radiation above the pool for controlling and regulating fusion welding processes", Weld. Int., vol. 8, pp. 488-491, 1994.
[11] F. Rizhkov, A. Bashkatov, A. Zakomoldin, V. Korneyev, "Welding of bronze BrH-08 and steel EI-811 with and oscillating electron beam", Automatic welding, vol. 5, pp. 56-58, 1973.
[12] N. Galchenko, S. Belyuk, K. Kolesnikova, "Study of the possibility of electron beam welding of a lance nozzle for oxygen converter steel production. Technology and equipment for electron beam welding", Proceedings of the International scientific and technical conference, Saint Petersburg, devoted to the 50th anniversary of space exploration and the 100th anniversary of the Center of the Materials Research Institute, pp. 150-157, 2011.
[13] L. Goncharov, E. Terentyev, A. Marchenkov, M. Portnov, "Electron beam welding of bronzes to 316 L(N) steel", Electrotechnica & Electronica, vol. 5-6, pp. 123-127, 2012.
[14] T. DebRoy, "Physical processes in fusion welding", Rev. Mod. Phys., vol. 1(67), pp. 85-112, 1995.
[15] Corresponding standard 5632-72, URL: http://pmkprogress.ru/wp-content/uploads/5632-72.pdf, (15.05.2015).
[16] Corresponding standard 28873-90. URL: http://metallicheckiy-portal.ru/marki_metallov/cup/BrX, (15.05.2015).
[17] E. Turkdogan, "Physical chemistry of high temperature processes". - Moscow: Metallurgy, 1985.
[18] S. Popel, V. Pavlov, O. Yesin, "Calculation of the surface tension of liquids by the excessive Helmholtz thermodynamic potential", Molecular liquids. Journal of physical chemistry, vol. 3(37), pp. 622-627, 1963.
[19] X. He, P. Fuerschbach, T. DebRoy, "Heat transfer and fluid flow during laser spot welding of 304 stainless steel", Journal of Physics (D): Applied Physics, vol. 12(36), pp. 1388, 2003.
[20] T. Olshanskaya, G. Permyakov, V. Belenkiy, D. Trushnikov, "Influence of Electron Beam's Oscillations on Weld's Structure Formation of Dissimilar Materials on an Example Steel with Bronze", Electrotechnica & Electronica, vol. 5-6(49), pp. 97-102, 2014.
[21] R. Rai, T. Palmer, J. Elmer, T. DebRoy, "Heat transfer and fluid flow during electron beam welding of 304L stainless steel alloy, Weld. J., vol. 88(3), pp. 54-61, 2009.
[22] V. Yazovskikh, V. Utochkin, "Thermodynamic evaluation of the relation of evaporation temperature and steam pressure in the keyhole during electron beam welding", Physics and Chemistry of Materials Treatment, vol. 2, pp. 73, 1997.